

Fully-electrodynamic radio simulations with Eisvogel

Philipp Windischhofer,^{a,*} Cosmin Deaconu^b and Christoph Welling^b

^aUniversity of Chicago, Enrico Fermi Institute, Kavli Institute for Cosmological Physics,
Chicago, IL 60637

^bUniversity of Chicago, Astronomy & Astrophysics, Kavli Institute for Cosmological Physics,
Chicago, IL 60637

E-mail: windischhofer@uchicago.edu, cozzyd@kicp.uchicago.edu,
christophwelling@uchicago.edu

Radio neutrino detection experiments require high-fidelity simulations to predict expected signal shapes and characterize backgrounds in the presence of complicated material geometries. This note describes recent progress in the development of *Eisvogel*, an open community tool that leverages electrodynamic Green's functions to enable efficient first-principles calculations of antenna signals in radio particle detectors. Emphasis is put on a description of the software architecture developed for the calculation and storage of large-scale Green's functions in a distributed-computing environment, on an exposition of wave-optics phenomena relevant for in-ice neutrino observatories, and a summary of progress towards end-to-end radio simulations using CORSIKA 8.

10th International Workshop on Acoustic and Radio EeV Neutrino Detection Activities (ARENA2024)

11-14 June 2024

The Kavli Institute for Cosmological Physics, Chicago, IL, USA

*Speaker

1. Introduction

Radio particle detection experiments require a thorough understanding of the creation, propagation, and detection of the electromagnetic emission from particle cascades developing in the instrumented material volume. This is particularly challenging for in-ice neutrino telescopes, which aim to detect ultra-high energy neutrinos through the radio signature of charged-particle showers initiated in the dense glacial ice of the Arctic or the Antarctic. The simulation of radio propagation through this medium is often done in the zero-wavelength limit of geometric optics, where the radio emission propagates along smooth “rays” from the shower to the receiver. However, realistic ice geometries typically involve features that are of a similar size as the wavelengths targeted by existing and planned experiments, and can thus support phenomena where finite-wavelength effects are important.

Fully capturing all such effects requires, in principle, solving Maxwell’s equations over the entire instrumented ice volume, where the signal-generating charged-particle shower is included as a source current distribution and the environment is represented by an arbitrary position- and frequency-dependent distribution of permittivity, permeability, and conductivity.

Eisvogel is an open community tool [1], currently under development, designed to address this general electrodynamic signal propagation problem in a computationally efficient manner. The principles on which the implementation is based have previously been introduced in Refs. [2–4]. They are briefly recapitulated in Section 2. Section 3 then gives a more detailed overview of the individual components of the *Eisvogel* implementation, focusing on recent progress in applying this framework to in-ice neutrino observatories. Finally, Section 4 provides an outlook on future developments.

2. Methodology

Eisvogel calculates the time-domain voltage signal $V_{\text{sig}}(t)$ that appears across the terminals of a receiving antenna as the result of an arbitrary electric current density $\mathbf{J}(\mathbf{x}, t)$ that is present in the simulation volume (representing the moving net electric charge in the shower front). This calculation is performed in two steps (cf. Figure 1), designed to be computationally efficient for the typical case where one is interested in simulating signals from many showers with different orientations and energies in the same environment.

First, a Green’s function for the antenna signal is derived and stored on disk. As explained in Refs. [2–4], Lorentz reciprocity identifies the Green’s function with the electric field configuration $\mathbf{K}(\mathbf{x}, t)$ that is attained if a Dirac-delta like current, suitably band-limited, is applied to the terminals of the antenna. Crucially, the Green’s function depends only on the properties of the antenna and the environment and this (generally expensive) calculation need only be performed once for every antenna and environment configuration of interest.

Second, the antenna signal for a particular shower realization is obtained by convolving the Green’s function with the shower current distribution,

$$V_{\text{sig}}(t) = - \int d^3\mathbf{x}' dt' \mathbf{K}(\mathbf{x}', t - t') \cdot \mathbf{J}(\mathbf{x}', t'). \quad (1)$$

(The overall minus sign in this expression is of no physical relevance and chosen by convention.)

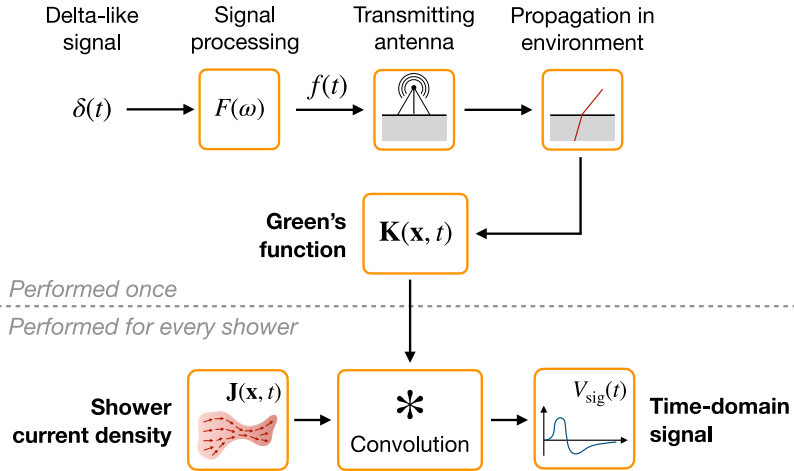


Figure 1: Architecture of *Eisvogel*, including the calculation of the Green’s function $K(x, t)$ for a given antenna and environment (top half) as well as the convolution of this Green’s function against the shower current distribution to yield the received time-domain antenna signal (bottom half).

3. Code architecture

The following gives a more detailed account of the calculation of the electrodynamic Green’s function (Section 3.1), the strategy developed for scalable on-disk storage (Section 3.2), and the integration of the shower signal calculation into the simulation framework CORSIKA 8 (Section 3.3).

3.1 Calculation of the electrodynamic Green’s function

Eisvogel interfaces with the open-source finite-difference time-domain (FDTD) solver MEEP [5] to allow electrodynamic Green’s functions to be calculated for arbitrary material distributions in the large-scale simulation volumes required to model in-ice detectors. For the common case of an (approximately) cylindrically-symmetric antenna in a cylindrically-symmetric medium, MEEP can directly solve Maxwell’s equations in cylindrical coordinates, greatly reducing the computational effort required. To cover the required large simulation volumes of $O(100 - 500 \text{ m})$ in linear scale at simultaneously much shorter wavelengths of $O(1 \text{ m})$, the FDTD calculation is run in a multi-processor environment utilizing MPI [6].

Figure 2 shows the time evolution of the electrodynamic Green’s function for an infinitesimal dipole antenna placed at a depth of approximately 30 m in a cylindrically-symmetric ice medium. The depth profile of the index of refraction is chosen to be a smooth three-stage piecewise-exponential function, as motivated from glaciological studies [7]. Additional depth-dependent index perturbations of at most $O(5\%)$ are applied to represent the seasonal density fluctuations known to exist in the firn [8].

By construction, the Green’s function has the character of an outgoing wave emitted by the antenna, part of which couples into the air or is reflected at the ice–air interface. Rapid density perturbations in the firn lead to a quasi-continuous series of partial reflections of the in-ice wave, effectively dispersing the initially sharp wavefront. There also exists a surface mode that propagates at the speed of light in air and couples back into the ice (sometimes referred to as “head wave”). It is responsible for the first-arrival of the signal in a large part of the shallow portion of the ice.

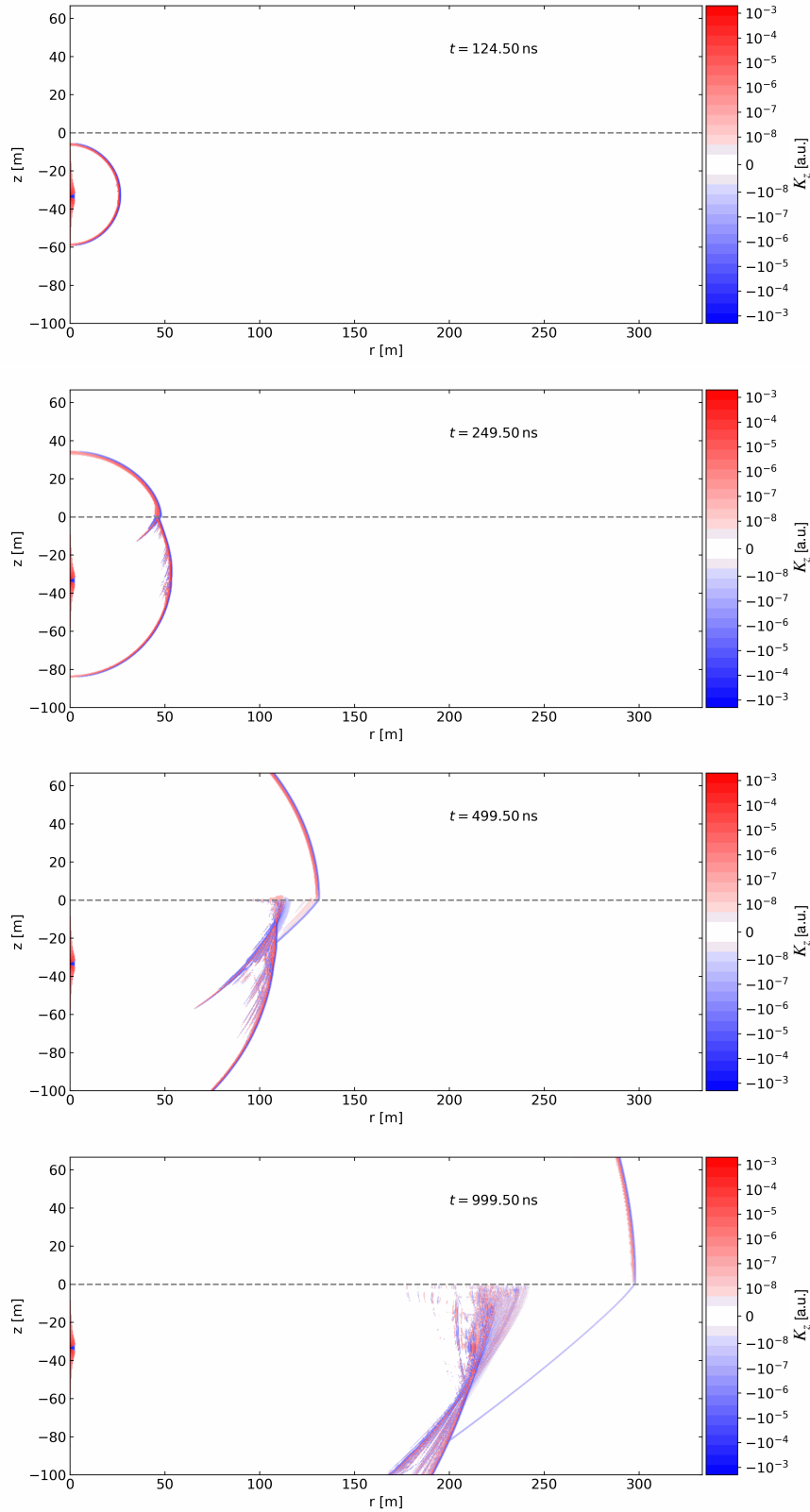


Figure 2: Time evolution of the vertical component $K_z(r, z, t)$ of the Green's function (top to bottom) for a vertically-polarized (infinitesimal) dipole antenna placed at a depth of approximately 30 m in a cylindrically-symmetric material distribution ($z > 0$: air with an index of refraction of unity, $z \leq 0$: ice with a depth-dependent index of refraction profile as described in the main text).

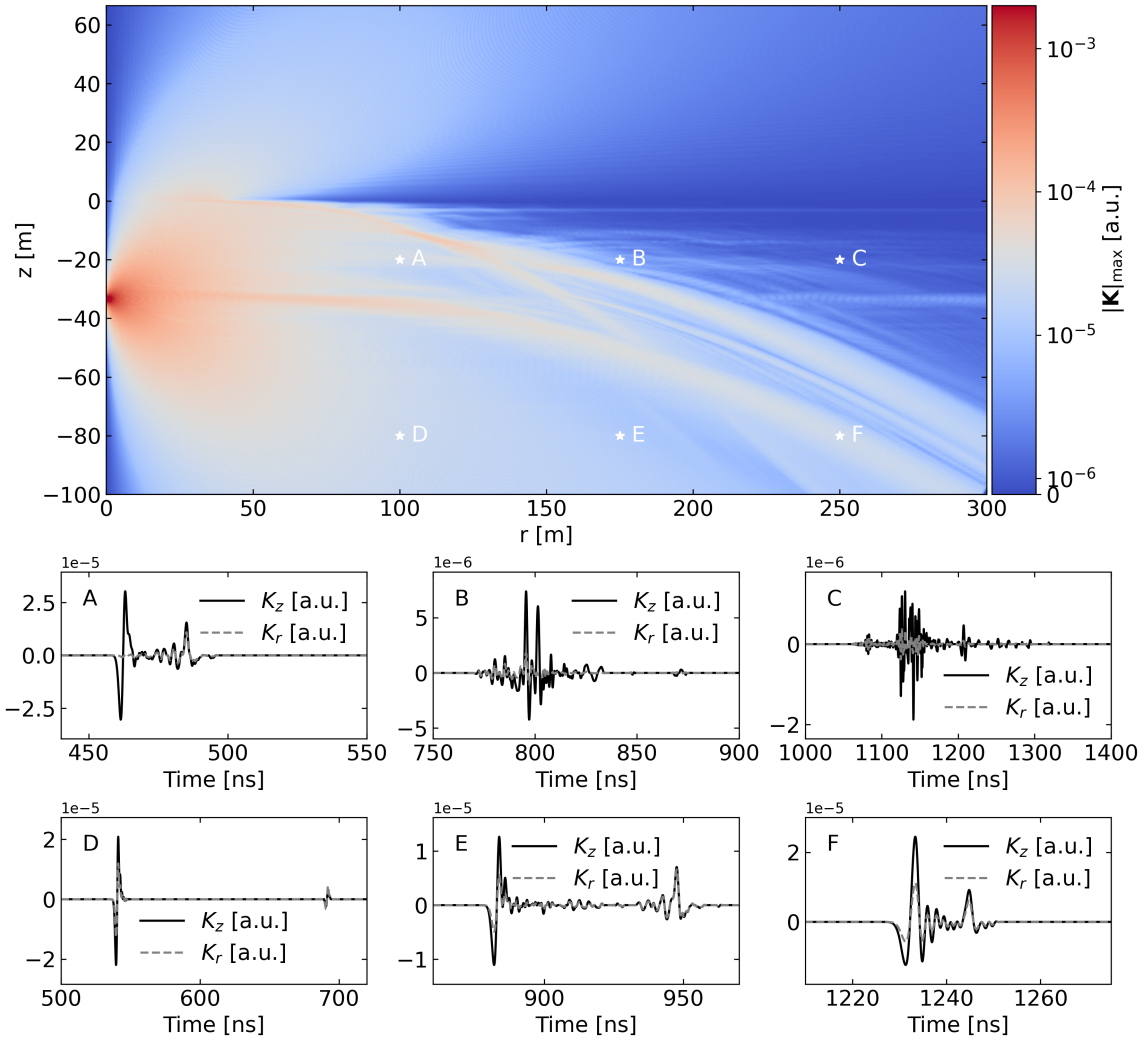


Figure 3: Top panel: Maximum instantaneous magnitude $|\mathbf{K}|_{\max}(\mathbf{x}) = \max_t |\mathbf{K}(\mathbf{x}, t)|$ of the Green's function for the same situation as Figure 2. Bottom panels: Evolution of the vertical component K_z and the radial component K_r of the Green's function at the spatial locations marked by A–F.

Figure 2 also shows the electrostatic component of the Green's function as a persistent structure located in the near field of the antenna, which, upon convolution with the shower current, generates the near-DC content of the antenna signal. For a signal chain with band-pass characteristics, this component is absent.

Figure 3 shows a different visualization of the Green's function for the same situation. It clearly shows the emergence of wave guide-like structures as a result of density perturbations in the ice that can channel the outgoing radiation field and generate significantly different intensities at nearby locations.

3.2 On-disk storage of the Green's function

As Figure 2 shows, the Green's function is extremely sparse in the time domain. Large field values are attained along the wavefronts, with the intensity throughout much of the remainder of

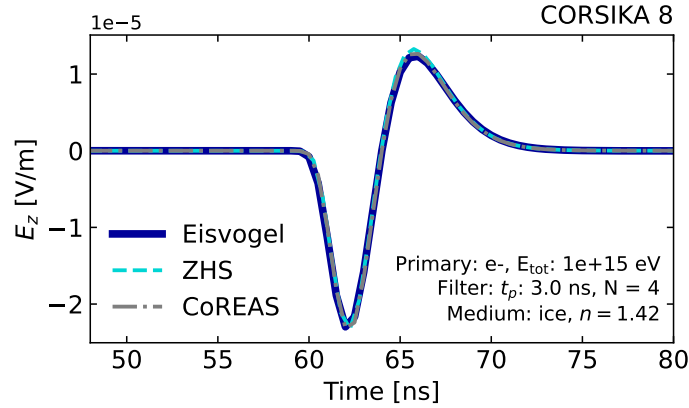


Figure 4: Comparison of the vertical electric field $E_z(t)$ observed by an infinitesimal dipole antenna, as calculated by *Eisvogel* (blue solid), ZHS [12] (cyan dashed), and CoREAS [13] (gray dash-dotted) for an electron-initiated shower ($E = 10^{15}$ eV) developing in a homogeneous medium with a refractive index of 1.42. The signals from all algorithms are band-limited by a 4th-order low-pass filter with a peaking time of $t_p = 3$ ns [2].

the simulation volume being significantly smaller. The Green’s function can thus be efficiently serialized to disk by limiting the dynamic range of the field content, i.e. by suppressing any field values $|\mathbf{K}(\mathbf{x}, t)|$ that are smaller than $\max_{t' < t} |\mathbf{K}(\mathbf{x}, t')|/d$, where d is the required dynamic range in the stored Green’s function. Values of $d \sim 10^2$ have been found to work well in initial example applications.

To enable efficient random access into the on-disk representation of the Green’s function, the simulation domain is partitioned into a number of rectangular “chunks”. The field content of each chunk is serialized into a separate file, and chunks consisting exclusively of suppressed field values are not serialized at all. All chunks are registered into an “index” that maps field coordinates into their respective on-disk locations. The index is built around an R^* tree [9], which is optimized [10] for efficient spatial lookup.

3.3 Application of the Green’s function

The numerical calculation of the antenna signal according to Eq. 1 requires the evaluation of the (band-limited) Green’s function at arbitrary locations. By default, *Eisvogel* uses a cubic kernel to interpolate between neighboring voxels, as explained in Ref. [4]. This flexible evaluation scheme supports a wide range of different forms for the (shower) current density \mathbf{J} , making it possible to base the signal calculation on quasi one-dimensional parameterized charge-excess profiles or microscopic shower simulations.

In particular, *Eisvogel* interfaces with CORSIKA 8 [11] to make the accurate calculation of shower radio signals in fully general media tractable for the first time. The ability of CORSIKA 8 to run multiple independent radio emission calculations simultaneously for the same shower is crucial to efficiently benchmark different approaches against the electrodynamically-correct result and study and delineate their respective regimes of validity. Figure 4 compares the *Eisvogel* calculation of the antenna signal with ZHS [12] and CoREAS [13] for a shower in a homogeneous medium, where the latter two algorithms are known to be accurate. Excellent agreement is observed between all

three codes, serving as an important initial confirmation and the starting point of a more in-depth validation campaign.

4. Conclusions and outlook

Eisvogel is a numerical code for the efficient calculation of radio emissions from charged-particle cascades and the propagation of this radiation through complex material geometries. An electrodynamic Green's function acts as the central element of the code, encoding the complex details of radiation propagation and thus making electrodynamically-correct signal calculations tractable for the first time.

To make the calculation of realistic Green's functions possible for the large volumes instrumented by radio particle detection experiments, *Eisvogel* integrates with the open-source Maxwell solver MEEP, and a custom file format has been developed for scalable on-disk storage. To enable a seamless end-to-end simulation of shower radio signatures in complex media, *Eisvogel* integrates with CORSIKA 8.

These new simulation capabilities have the potential to significantly improve the understanding of current and future experiments targeting ultra-high energy neutrinos or charged cosmic rays. Beside in-ice neutrino observatories, potential applications of *Eisvogel* include highly-inclined air showers and air shower emissions in anomalous atmospheric conditions, tau neutrino detection, as well as first-principles noise temperature calculations for antennas embedded in complex media.

References

- [1] P. Windischhofer, C. Welling, C. Deaconu, *Eisvogel* code repository, <https://github.com/eisvogel-project/Eisvogel> (visited on 05/08/2024)
- [2] W. Riegler, P. Windischhofer, "Signals induced on electrodes by moving charges, a general theorem for Maxwell's equations based on Lorentz-reciprocity", Nucl. Instrum. Meth. A, 980, 164471 (2020)
- [3] P. Windischhofer, W. Riegler, "Electrical signals induced in detectors by cosmic rays: a reciprocal look at electrodynamics", PoS(ICRC2021), 184 (2021)
- [4] P. Windischhofer, C. Welling, C. Deaconu, "Eisvogel: Exact and efficient calculations of radio emissions from in-ice neutrino showers", PoS(ICRC2023), 1157 (2023)
- [5] A. F. Oskooi, D. Roundy, M. Ibanescu, P. Bermel, J. D. Joannopoulos, S. G. Johnson, "Meep: A flexible free-software package for electromagnetic simulations by the FDTD method", Comput. Phys. Commun. 181, 687–702 (2010)
- [6] Message Passing Interface Forum. "MPI: A Message-Passing Interface Standard, Version 4.1", Last retrieved 2024-08-06, <https://www.mpi-forum.org/docs/mpi-4.1/mpi41-report.pdf>
- [7] K. Couberly and the ARA Collaboration, "Modeling the refractive index profile $n(z)$ of polar ice for ultra-high energy neutrino experiments", arXiv:2406.00857 [astro-ph] (2024)

- [8] C. M. Stevens, V. Verjans, J. M. D. Lundin, E. C. Kahle, A. N. Horlings, B. I. Horlings, E. D. Waddington, “The Community Firm Model (CFM) v1.0”, *Geosci. Model Dev.*, 13, 4355–4377 (2020)
- [9] N. Beckmann, H. P. Kriegel, “The R^* -tree: An efficient and robust access method for points and rectangles”, *SIGMOD Rec.* 19, 2, 322–331 (1990)
- [10] S. T. Leutenegger, M. A. Lopez, J. Edgington, “STR: a simple and efficient algorithm for R-tree packing”, *Proceedings of the 13th International Conference on Data Engineering*, Birmingham, UK, 497-506 (1997)
- [11] R. Engel, D. Heck, T. Huege, et al., “Towards a Next Generation of CORSIKA: A Framework for the Simulation of Particle Cascades in Astroparticle Physics”, *Comput. Softw. Big Sci.* 3, 1 (2019)
- [12] J. Alvarez-Muniz, A. Romero-Wolf, E. Zas, “Cherenkov radio pulses from electromagnetic showers in the time-domain”, *Phys. Rev. D* 81, 123009 (2010)
- [13] T. Huege, M. Ludwig, C. W. James, “Simulating radio emission from air showers with CoREAS”, *AIP Conf. Proc.* 1535, 128 (2013)